JOURNAL OF MATERIALS SCIENCE **35** (2000) 6209–6212

Preparation of epitaxially grown $LaSrCoO_3$ thin films on $SrTiO_3(100)$ substrates by the dipping-pyrolysis process

KYU-SEOG HWANG, HYUNG-MIN LEE
School of General Education, Nambu University, 864-1 Wolgyedong, Kwangsanku, Kwangju 506-302, South Korea
E-mail: khwang@mail.nambu.ac.kr

YONG-MU LIM
Department of Ophthalmic Optics, Kwangju Health College, 638-8 Shinchangdong, Kwangsanku, Kwangju 506-306, South Korea

$LaSrCoO_3$ thin films were spin-coated onto $SrTiO_3(100)$ substrates by the dipping-pyrolysis process. X-ray diffraction θ-2θ scans and X-ray diffraction β scans were used to determine the crystallinity and in-plane alignment behavior of the films. The X-ray diffraction pattern shows the film obtained by annealing at 800°C was highly oriented. The X-ray diffraction pole-figure analysis and reciprocal-space mapping (ω-2θ scans) of the resulting film showed that the film comprising the pseudocubic phase had an epitaxial relationship with the $SrTiO_3$ substrate. © *2000 Kluwer Academic Publishers*

1. Introduction

Pt or Pt-based metal films are often used as bottom electrodes in the fabrication of integrated ferroelectronic capacitors for memory applications; however, their performance against fatigue is unsatisfactory [1]. Recently, conductive perovskite oxides such as $YBa_2Cu_3O_{7-\sigma}$, $SrRuO_3$, IrO_2 and $LaNiO_3$ [2–5] have been studied intensively as electrodes. $LaSrCoO_3$ (LSCO), which is a perovskite related metallic oxide [6, 7], has also attracted much attention in recent years, as a conduction layer for application in ferroelectric memories. The pseudocubic "*a*" of this oxide is 0.3835 nm [8]. Because LSCO has a structure similar to that of perovskite ferroelectrics, textured and epitaxially grown LSCO film is a promising oxide electrode.

At present, most epitaxial LSCO films have been prepared by physical processes such as pulsed laser deposition (PLD) [7, 9] and rf magnetron sputtering [10]. A chemical solution process provides a simple and versatile alternative for crystalline thin film preparation [11, 12]. However, so far as we know, very few works on the preparation of epitaxial or textured LSCO thin films by a chemical solution process have been reported.

In this work, we report on the fabrication of epitaxially grown LSCO thin films on $SrTiO_3(100)$ (STO) substrates by the dipping-pyrolysis (DP) process.

2. Experimental

The method used to prepare LSCO thin films was similar to that of $Pb(Zr,Ti)O_3$ films described in our previous paper [11]. La-nitrate [$La(NO_3)_3{\cdot}6H_2O$], Sr-chloride ($SrCl_2{\cdot}6H_2O$) and Co-nitrate [$Co(NO_3)_2{\cdot}6H_2O$] with a La : Sr : Co molar ratio of 1 : 1 : 2 were used as starting materials. They were dissolved and diluted with ethylene glycol monomethyl ether ($CH_3OCH_2CH_2OH$) to achieve an appropriate concentration and viscosity for deposition of smooth films by spin coating (concentration: 212.3 mg metal/ml coating solution). Generally, solutions prepared by inorganic metal salts are very stable in air and there is no chemical reaction upon mixing or dilution, in contrast to metal alkoxide solutions, which are commonly used in chemical solution processes.

Single crystal STO(100) was used as the substrate. It was cleaned in neutral solution, then immersed in H_2O_2 solution, and finally rinsed in acetone. The starting solution was spin coated onto the cleaned substrate at 4000 rpm for 10 sec in air. After each coating, the film was dried at 110°C for 30 min in air and prefired at 500°C for 10 min in air. The process was repeated 3 times to prepare a thicker layer of LSCO. The films studied were typically $0.7 \sim 0.8$ μm thick, which was confirmed by weight gain and by observation of the fracture cross section of the films using scanning electron microscopy (SEM) (JEOL JSH-5400). Final annealing was carried out in air at 800°C for 1 hr. The crystallinity and in-plane alignment of the annealed films were examined by X-ray diffraction (XRD) (MAC Science MXP^{3A}) θ-2θ scans, pole-figure analysis (β scans) and reciprocal-space mapping ($2\theta/\Delta\omega$ scan) by the Schulz reflection method using Cu Kα radiation. Resistivity was measured by the four-probe method, and the free surface of the film was characterized by SEM.

3. Results and discussion

Fig. 1 shows the XRD patterns of LSCO thin films on STO(100) substrates prefired at (a) 500°C and annealed at (b) 800°C. As shown in Fig. 1b, a single phase LSCO film with high orientation was observed in the XRD θ-2θ scans, thus, amorphous precursor films were crystallized after the final annealing at 800°C. The (110) reflection, corresponding to the strongest peak in LSCO powder diffraction or non-oriented LSCO grains, was not detected; this means that the films are highly oriented.

Using the STO peak as an internal calibration standard, the lattice parameter $d_\perp$ of LSCO film perpendicular to the substrate surface in Fig. 1b was determined to be 0.382 nm. The $d_\perp$ value of highly oriented film annealed at 800°C on STO is smaller than that of bulk crystal ($a/\sqrt{2} = 0.3835$ nm) and this may be due to the tensile stress along the a/b-axis resulting from the lattice mismatch between LSCO and STO ($a = 0.3905$ nm).

To investigate the in-plane alignment of the highly oriented LSCO film annealed at 800°C, we performed XRD pole-figure analysis using the Schulz reflection method. We choose the LSCO(220)/(202) reflection for study because of its high intensity and separation from the STO substrate reflection. Fig. 2 shows the (220)/(202)-pole-figure for film on STO annealed at 800°C. After setting the 2θ at 69.46°, which corresponds to the LSCO(220)/(202) reflection, the film was rotated from $\beta = 0°$ to $\beta = 360°$ at the tilt angle of $\alpha = 30°$ to $\alpha = 60°$. As shown in Fig. 2, the four sharp spots of the LSCO(220)/(202) reflection were observed at every 90° and the β angles of these spots agreed with those for the STO(220) reflection not shown here. The full-widths at half maximum (FWHM) of the peaks along β direction were 1.6°. The comparison of these peak positions with those for the STO substrate indicates an epitaxial relationship between the LSCO and the STO in which LSCO[100] aligns with both [001] and [010] directions of STO substrate.

Further, to evaluate crystal structure and the lattice constants along the in-plane directions of the LSCO film on the STO substrate, reciprocal-space mapping was measured for the film annealed at 800°C by asymmetric XRD $2\theta/\omega$ scans. In this paper, the θ- and ω-angles refer to symmetric and asymmetric

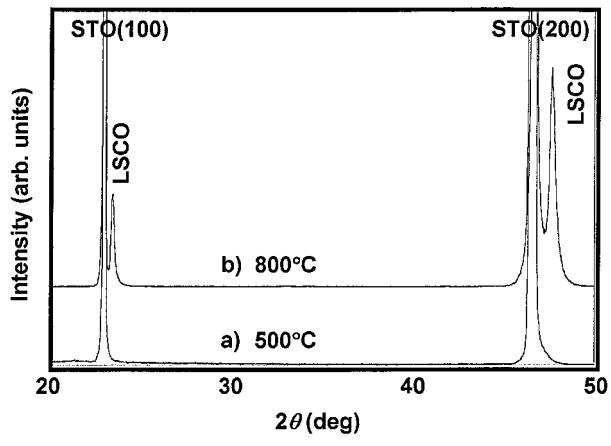

Figure 1 XRD θ-2θ scans for the LSCO/STO (a) prefired at 500°C and (b) annealed at 800°C.

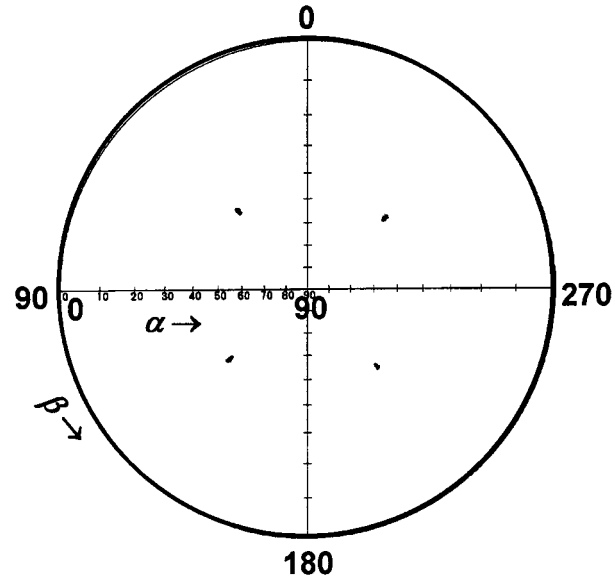

Figure 2 Pole figure of (220)/(202) reflection for the LSCO/STO annealed at 800°C.

Bragg reflections, reflectively; their rotation axes are the same. Fig. 3a and b show a bird's eye view and a contour, respectively, of the resulting $2\theta/\omega$ maps. A strong peak derived from the substrate of STO(330) reflection at $2\theta = 113.63°$ and a small peak derived from LSCO(330) reflection of the epitaxial film at $2\theta = 117.13°$ are recognized in these mapping graphs.

Fig. 4a–c show three schematic illustrations of the alignment of epitaxial LSCO grains on the STO(100)

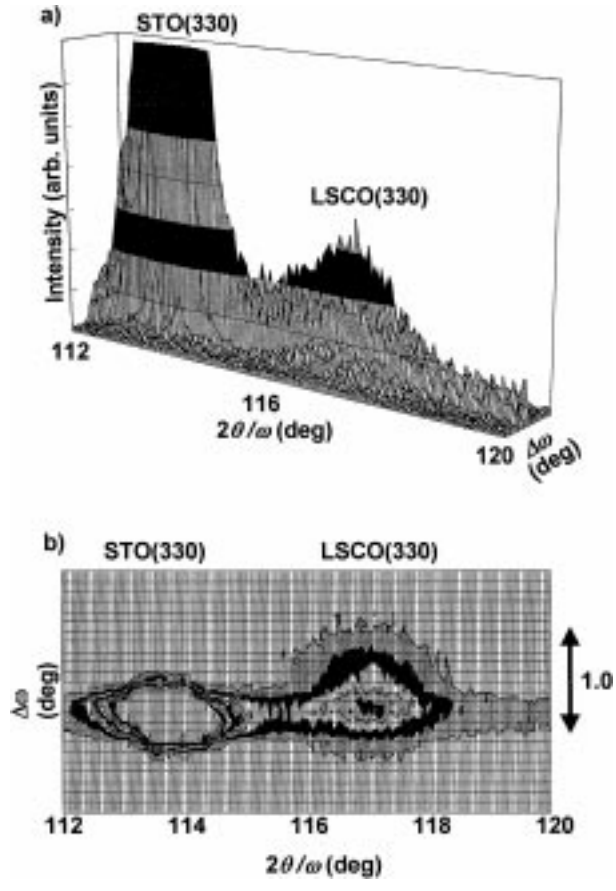

Figure 3 A bird's eye view (a) and a contour (b) of XRD reciprocal-space ($2\theta/\omega$ vs. $\Delta\omega$) mapping for an epitaxial LSCO film on STO(100) substrate.

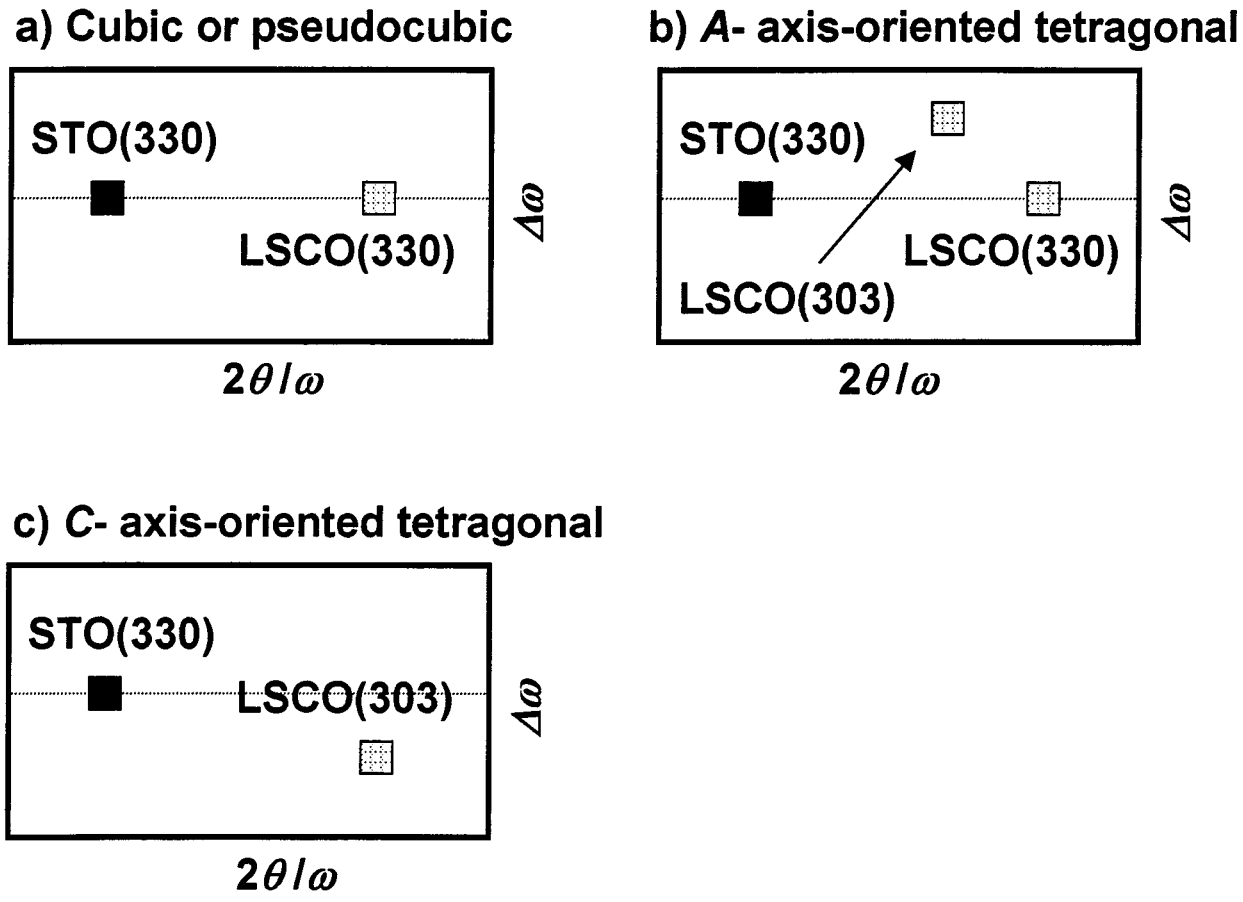

Figure 4 Schematic illustrations of three possible configurations for epitaxial LSCO film on STO(100).

substrate, together with the corresponding reciprocal-space maps: (a) cubic or pseudo-cubic LSCO, (b) *a*-axis-oriented tetragonal LSCO, and (c) *c*-axis-oriented tetragonal LSCO. Firstly, if the LSCO phase has a cubic or pseudo-cubic structure, only one spot corresponding to LSCO(330) should appear on the same horizontal line of $\Delta\omega$ as that of STO(330) [Fig. 4a]. Secondly, if the LSCO is in the *a*-axis-oriented tetragonal phase ($a_f < c_f$), there are two possible alignments, corresponding to so-called 90° domain structure, thus, two spots should be observed in the map as shown in Fig. 4b. Finally, if the LSCO is in the *c*-axis-oriented tetragonal phase ($c_f > a_f$), only one spot is expected to occur below the horizontal line of $\Delta\omega$ which runs through that of STO(330) [Fig. 4c]. Note that, when $c_f > a_f$, the LSCO(303) peak occurs above the horizontal line of $\Delta\omega$ for the *a*-axis orientation while it occurs below the horizontal line of $\Delta\omega$ for the *c*-axis orientation. The relative locations of the two spots, corresponding to LSCO and STO annealed at 800°C agree with those in Fig. 4a, indicating that the LSCO has a pseudo-cubic phase.

From the lattice constant $d_\perp = 0.382$ nm calculated earlier by XRD θ-2θ scans and the position of peak top of LSCO(330) and STO(330), the lattice constant ($d_\parallel$) of the LSCO along one of the in-plane directions was calculated to be 0.384 nm. The $d_\perp$ value of the film is smaller than that of bulk pseudocubic LSCO and the $d_\parallel$ value of present film. However, $d_\parallel/d_\perp$ ratio of the film is 1.005, which is similar to 1 of the bulk pseudocubic LSCO. Thus our film is considered to be epitaxially grown pseudocubic LSCO film.

In order to explain the epitaxial growth in our film, we illustrated atomic ion frame works and lattice constants of LSCO(100) and STO(100). As shown in Fig. 5a and b, the small lattice-mismatch between the LSCO ($a/\sqrt{2} = 0.3835$ nm) and STO may favor the epitaxial growth. Further, we assume that compressive film stress, primarily due to the tensile stress along the in-plane directions, causes smaller $d_\perp$ value.

Fig. 6 shows a plot of resistivity vs. temperature for the LSCO film annealed at 800°C. The temperature dependence ($d\rho/dT$), i. e., ρ_{300K}/ρ_{100K} of the LSCO film on STO was about 1.14, indicates metallic behavior, which is important for electrode application. However, the resistivity of the film at room temperature is 12.3×10^{-3} Ω·cm, this value is very higher than the value of 90 μΩ·cm of a bulk LSCO. The increase of the resistivity may be due to the stress along the *c*-axis because the lattice constant of the STO is larger than that of LSCO. Moreover, as shown in Fig. 7, the free surface of the LSCO film exhibited a typical polycrystalline texture with some pores. Generally, in the chemical solution method, pores and cracks are easily recognized in the product films. The pore distribution in the film will lead to an increase in the resistivity.

It should be noted that several reports on the preparation of "highly oriented" LSCO films by the chemical solution method have been published [13]. In those reports, however, the alignment of the films was discussed based only on the *d*-values determined from XRD θ-2θ scans. In our results, the epitaxial relationship and crystal structure of the LSCO were clearly confirmed

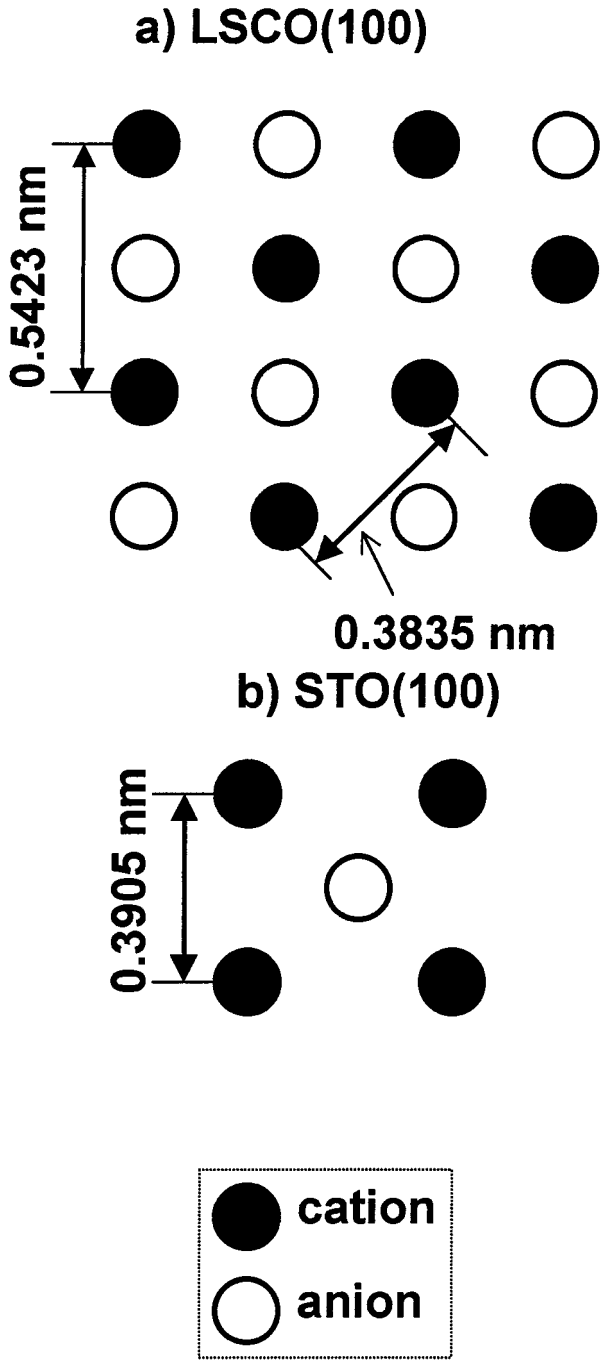

Figure 5 Atomic ion frame works and lattice constants of (a) the LSCO(100) and (b) the STO(100).

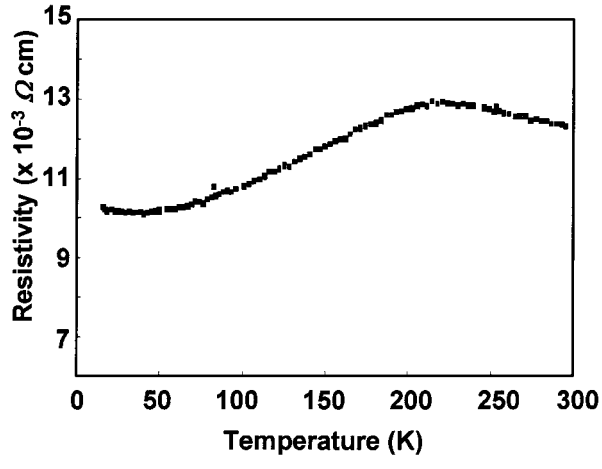

Figure 6 Resistivity vs. temperature for the LSCO/STO annealed at 800°C.

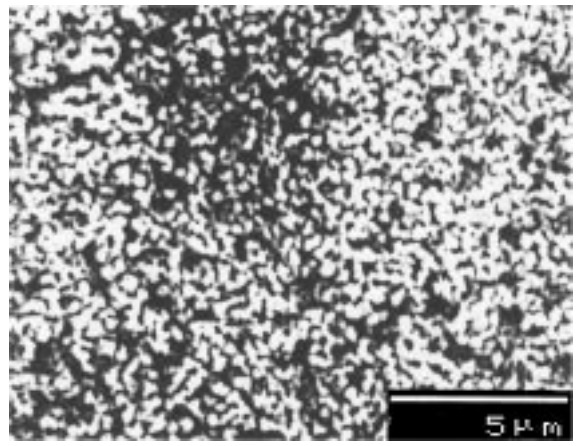

Figure 7 SEM photograph of the free surface of epitaxial LSCO film on STO substrate annealed at 800°C.

by XRD pole-figure analysis and reciprocal-space mapping study. Further research is required to decrease the resistivity of the epitaxial LSCO film.

4. Conclusion

LSCO films on STO(100) substrate were prepared by the DP process, using inorganic salts as the starting materials. Highly (*h*00)/(00*l*)-oriented LSCO film was obtained from spin-coated films prefired at 500°C and subsequently annealed at 800°C. Pole-figure analysis and reciprocal-space mapping indicated that the thin film comprising the pseudo-cubic phase have an epitaxial relationship with the STO substrate.

References

1. R. RAMESH, W. K. CHAN, B. WILKENS, H. GILCHRIST, T. SANDS, J. M. TARASCON, V. G. KERAMIDAS, D. K. FORK, J. LEE and A. SAFARI, *Appl. Phys. Lett.* **61** (1992) 1537.
2. J. LEE, L. JOHNSON, A. SAFARI, R. RAMESH, T. SANDS, H. GILCHRIST and V. G. KERAMIDAS, *ibid.* **63** (1993) 27.
3. C. B. EOM, R. B. VAN DOVER, J. M. PHILLIPS, D. J. WERDER, J. H. MARSHALL, C. H. CHEN, R. J. CAVA and R. M. FLEMING, *ibid.* **63** (1993) 2570.
4. K. TAKEMURA, T. SAKUMA and Y. MIYASAKA, *ibid.* **64** (1994) 2967.
5. K. P. RAJEEV, G. V. SHIVASHANKAR and A. K. RAYCHAUDHURI, *Solid State Commun.* **79** (1991) 591.
6. Z. L. WANG and J. ZHANG, *Phys. Rev. B* **54** (1996) 1153.
7. K. H. WONG, W. WU, P. W. CHAN and J. T. CHEUNG, *Thin Solid Films* **312** (1998) 7.
8. J. T. CHEUNG, P. E. D. MORGAN, D. H. LOWNDES, X.-Y. ZHENG and J. BREEN, *Appl. Phys. Lett.* **62** (1993) 2045.
9. A. M. DHOTE, S. MADHUKAR, W. WEI, T. VENKATESAN, R. RAMESH and C. M. COTELL, *ibid.* **68** (1996) 1350.
10. L. FAHUA, X. DINGQUAN, P. WENBIN, W. HONGTAO, Z. JIANGUO and Z. WEN, *J. Kor. Phys. Soc.* **32** (1998) S1471.
11. K. HWANG, T. MANABE, I. YAMAGUCHI, S. MIZUTA and T. KUMAGAI, *J. Ceram. Soc. Jpn.* **105** (1997) 952.
12. K. HWANG, T. MANABE, T. NAGAHAMA, I. YAMAGUCHI, T. KUMAGAI and S. MIZUTA, *Thin Solid Films* **347** (1999) 106.
13. F. WANG, A. UUSIMÄKI and S. LEPPÄVUORI, *Appl. Phys. Lett.* **67** (1995) 1692.

Received 30 March 1999
and accepted 25 May 2000